

RF - MEMS and its Applications to Microwave Systems, Antennas and Wireless Communications

Christos G. Christodoulou

Abstract- MEMS-based products combine both mechanical and electronic devices on a monolithic microchip to produce superior performance over solid-state components, especially for wireless applications. RF-MEMS components are mainly used as inductors, tunable capacitors, switches, in VCOs, and resonators. Popular MEMS switches for wireless applications include transmit/receive duplexers, band-mode selection, time delay for phased-array antennas, and reconfigurable antennas. This paper talks about the use of MEMS switches in conjunction of fractal antennas to achieve multi-frequency, reconfigurable antennas

that can be used for a variety of communication applications and how micromachining can be used to fabricate new 3-D MEMS antenna structures for very high frequency applications.

Index Terms – Re-configurable antennas, wideband, fractal, RF-MEMS

I. INTRODUCTION

A critical requirement of many miniature systems is the ability to sense and/or transmit electromagnetic energy for communications or remote sensing. This can be accomplished using radio-frequency (RF), microwave, or millimeter-wave antennas that can be fabricated monolithically with other electrical/mechanical components to yield a new class of reconfigurable antennas capable of multi-band operation, adaptive beamforming, jamming/interference mitigation, polarization diversity, low-observability, and direction of arrival estimation. By combining low-loss, high-isolation RF MEMS switches with resonant microstrip or fractal radiators, we can physically reconfigure antennas and their feed structures in order to provide frequency band and polarization diversity. The MEMS micro-relays are used to alternately connect or isolate sub-structures on the planar antenna element, creating a geometrically distinct radiator for each combination of switch positions.

In addition, MEMS [1-5] phase-shifters can be used in conjunction with multiple antenna elements to realize novel monolithic low-cost electronically steerable arrays (ESAs). These ESAs will facilitate future integration with active devices and signal processors to realize 'smart' antenna

systems capable of autonomous frequency-band and radiation pattern adaptation. This stands to revolutionize next generation satellite and terrestrial telecommunication systems, intelligent tags, and fusing radars.

In this work, RF MEMS are used in conjunction with fractal antenna structures as the basis of a new re-configurable antenna approach. This approach has not been attempted before to the best of our knowledge. In the past, re-configurable antennas have been restricted to the use of non-fractal elements. Here the use of fractals is mainly for multi-frequency applications. A fractal antenna can be designed to receive and transmit over a wide range of frequencies through the property of self-similarity at different physical scales [6,7].

The use of RF MEMS switches permits the overall fractal pattern to be dynamically "shattered" into subsets, some of which do not respond uniformly to the entire theoretic spectrum. This property may permit the spectral isolation of impinging RF energy through binary search algorithms. This agility offers enabling benefits for modern radar and telecommunication systems by permitting deliberate alterations in antenna performance to accommodate changes in mission, environment; tolerance to defects and faults; and enabling new algorithmic approaches and direct digital synthesis.

This new type of antenna system can be designed for protection and geo-location applications as well. The aim is to be able to adjust the radiation pattern for the required frequency of operation, polarization and mission in general.

The electromagnetic performance of the RF MEMS switches is considered almost ideal at the frequencies of interest and their placement is accomplished by small physical connections of the antenna's adjacent conducting parts. Several configurations have been studied and analyzed and some of the results are shown in the sections to follow herein. Moreover, examples of 3-Dimensional MEMS antennas that can be used for high frequency applications are presented and discussed.

II. FRACTAL ANTENNAS

Most fractal antennas, including the Sierpinski Gasket antenna, have been studied extensively over the last few years [8-12]. The Sierpinski Gasket antenna shown in Figure 1 is

C. G. Christodoulou is with the Electrical and Computer Engineering Department, The University of New Mexico, Albuquerque, NM 87131 (e-mail:christos@ece.unm.edu).

chosen for this paper. The selection was based on the antenna's multi-frequency performance, as its active shape can be altered in many different ways providing different current paths, frequency bands and radiation patterns. The antenna has a flare angle of 60° and provides constant radiation pattern all over its bandwidth. Each element's side-length is 2.7cm. The antenna is etched as a monopole on a duroid dielectric layer of 1.588mm thick, and relative dielectric permittivity $\epsilon_r=4.4$. The monopole is then placed vertically on a ground plane to create an image. It is then fed from the tip using a coaxial cable whose outer metal is connected to the ground plane and its inner conductor to the monopole itself.

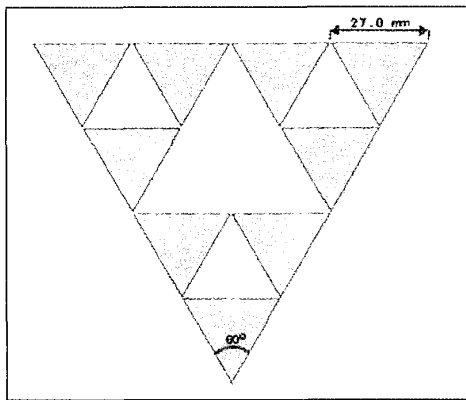


Figure 1. The design characteristics of the Sierpinski gasket antenna

The characteristics for this antenna without switches are shown in Figures 2(a) and 2 (b). The bandwidth is from 1.5GHz to 2.1GHz and the radiation pattern is similar to the printed dipole antenna, making it ideal for receiver use.

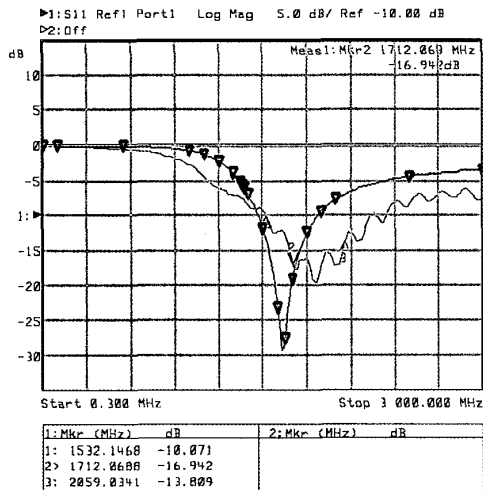


Figure 2 (a). S11 of the fractal antenna with all switches off (i.e. all parts of the fractal antenna are not connected to each other)

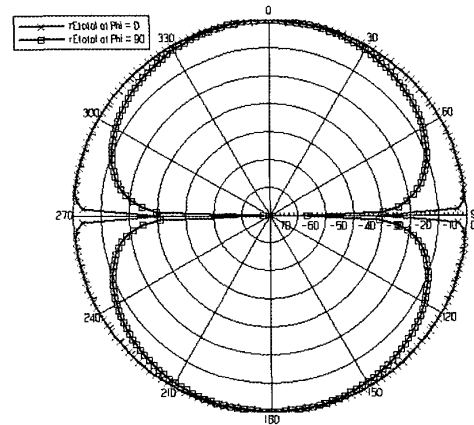


Figure 2 (b) the radiation pattern of a fractal antenna with all switches off.

III. ANTENNA AND SWITCH CONFIGURATIONS

In general, the coupling between the elements of a fractal antenna is very weak. Here we consider that the elements are connected with almost ideal switches. Therefore a switch conductively connects two adjacent antenna's elements when it is activated, changing the antenna's physical dimensions. Small gaps are created in the etched fractal antenna, which are bridged using MEMS switches.

The presence of the switches themselves has a very little effect on the performance of the antenna. Figure 3 depicts the physical layout of a typical RF MEMS CPW switch. The magnitude of the reflection coefficient S_{11} remains below -10dB all over the antenna's bandwidth as shown in Figure 4. Figure 4 also shown a comparison of experimental results of S_{11} and theoretical results. It should be mentioned here that these results are of the unpackaged switch. Figure 5 shows how a shunt MEMS switch operates. Figure 6, depicts the currents that flow from one side to the other when the switch is on.

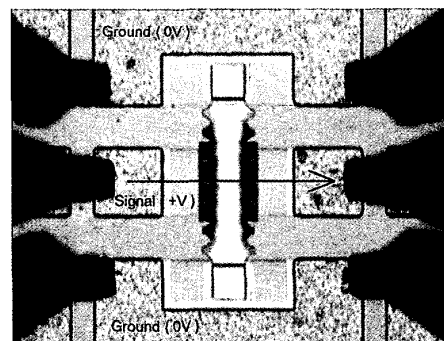


Figure 3. A CPW RF-MEMS switch

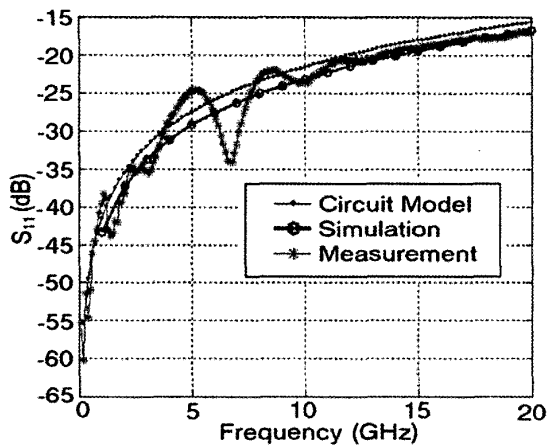


Figure 4. S_{11} for the MEMS switch in Figure 3

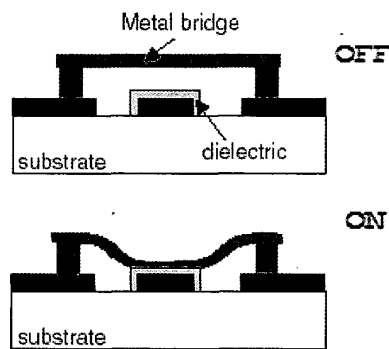


Figure 5. Side view of a shunt MEMS switch

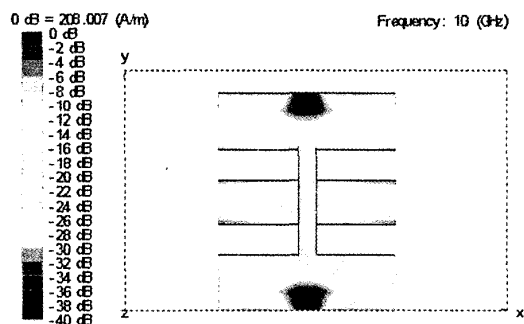


Figure 6. Simulated current on of the MEMS switch

Several cases were analyzed with the switches turned ON and OFF at different locations of the fractal antenna. First, the antenna was simulated with all switches set to ON (i.e. the antenna acted as regular fractal antenna with all of its conductive parts connected to each other). The currents on the antenna elements for this case and the reflection

coefficient response are shown in Figures 7(a) and 7(b). The coupling between the antenna's elements has drastically increased, compared to that in Figure 2(a). Also, additional resonant frequencies have been accomplished at frequencies below 2 GHz, as there are resonances at 0.55 GHz and 1.55 GHz.

As a second case, the far end switches are turned off, resulting in the smaller 1-iteration Sierpinski gasket antenna. As it was expected, the first resonance occurs at approximately 900 MHz, while the next is estimated around 3 GHz. The current flow and the radiation pattern is shown in Figure 8(a,b).

In the figures to follow, the elements with currents will be shown with blue color, while the inactive with gray. It is notable though that all the following configurations reveal a dipole-like radiation pattern at the first resonance, and a dipole-like radiation pattern with side-lobes at the next resonances. The active antenna region can be symmetric around the y-axis of the antenna, or non-symmetric. Also, it can be symmetric with respect to the ground plane as in Figure 11.

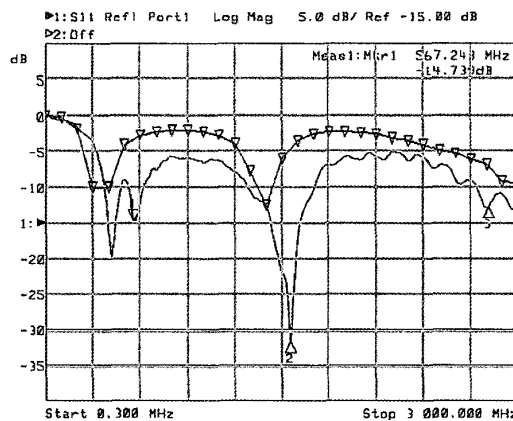
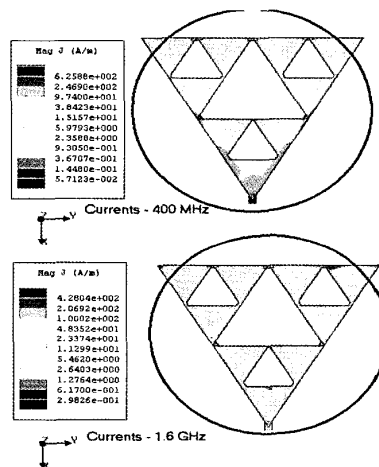


Figure 7(a,b). a) current flow on the antenna (circle shows the active region), b) the $|S_{11}|$ of the antenna.

By examining more possible configurations, we obtain a total of 14 resonant frequencies, 6 of which are below 1.7 GHz. These are namely at: 450MHz, 600MHz, 1.2GHz, 1.4GHz, 1.5 GHz and 1.6 GHz, and most with a dipole like radiation pattern. Basically, many other configurations can be established depending on the location of the ON or OFF switch. Each change of the switch will not only affect the currents on specific parts of the antenna but it will change its overall resonance performance and radiation pattern.

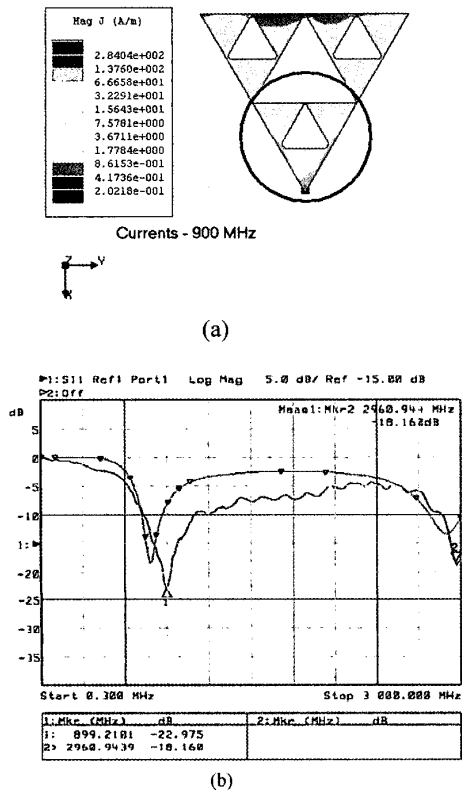
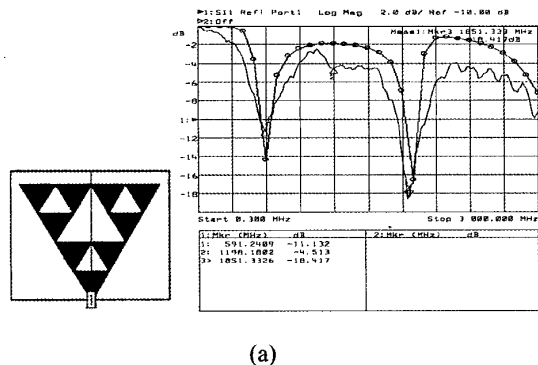
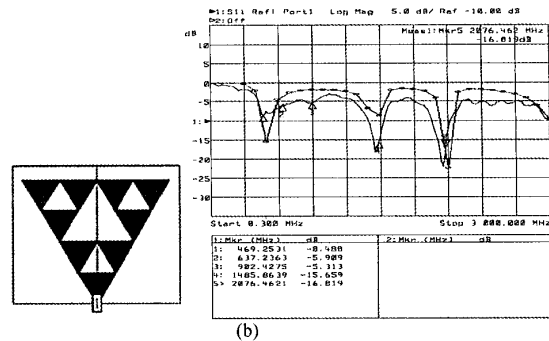


Figure 8 (a) current flow on the antenna (circle shows the active region), b) the S_{11} of the antenna



(a)



(b)

Figure 9(a,b). Symmetric re-configurable antenna structures and their corresponding $|S_{11}|$ response.

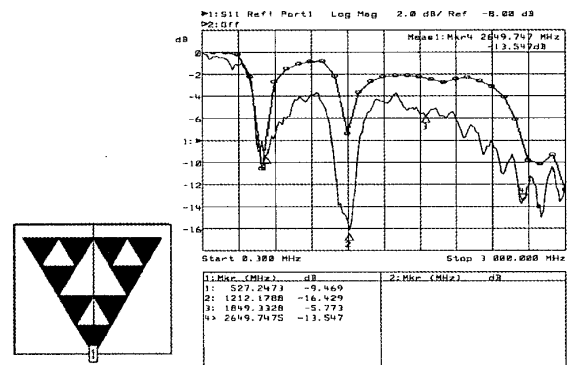


Figure 10. Non-symmetric re-configurable antenna structures and their corresponding $|S_{11}|$ response

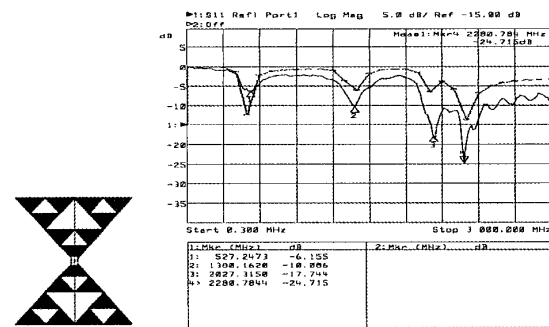


Figure 11. Symmetric with respect to the ground plane.

III. SERIES MEMS SWITCHES

Fractal antennas are generally placed as monopoles vertically over a ground plane. In our case, we need to etch the fractal antenna on the same layer with the series CPW RF-MEMS switch shown in Figure 12. Therefore the antenna needs to be etched on a layer of Silicon (silicon wafer). In order to achieve this, we etch a fractal dipole antenna (similar to the printed dipole), on a silicon dielectric with relative dielectric constant $\epsilon_r=11$. For manufacturing reasons the antenna has to fit in a quarter of a silicon wafer with 4"

diameter.

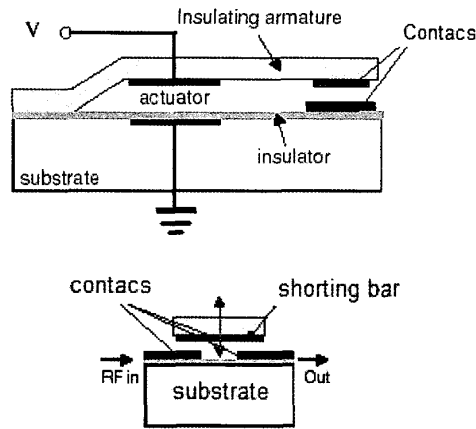


Figure 12. Side and front views of a series MEMS switch

Silicon etched antennas are easy to manufacture, and the CPW switches can also be easily etched. For our antenna the triangular patches were chosen to have side-length of 10mm. Also, a $140\mu\text{m}$ gap was placed between each patch in order for the switch to be etched there. The diagonal gap length was measured $138\mu\text{m}$ for this particular design, but a slight change in any of these lengths will not affect much the antenna's behavior, apart from the fact that increasing the size of the antenna decreases the resonant frequency.

It is worth noting that such a dielectric layer, with large thickness, can provide good matching for very broadband antennas. On the other hand, we need to comply with the design rules of our case where the dielectric has the thickness of a silicon wafer. The antenna has total dimensions 20.14×35.439 mm. Its highest resonance occurs at 4GHz as shown in Figure 14. We have therefore enough space to place the bottom left edge of the antenna 5×5 mm away from the center of the silicon wafer's disk (Figure 13).

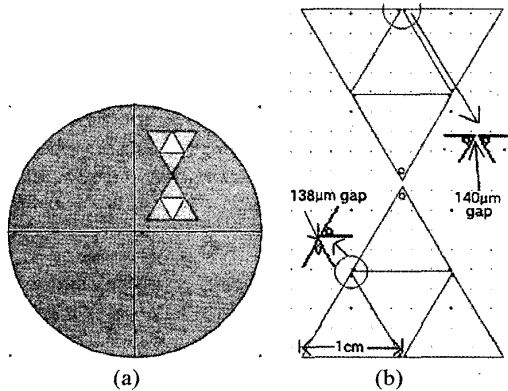


Figure 13. a) The antenna as etched on a quarter of a silicon wafer. b) The antenna's shape and dimensions.

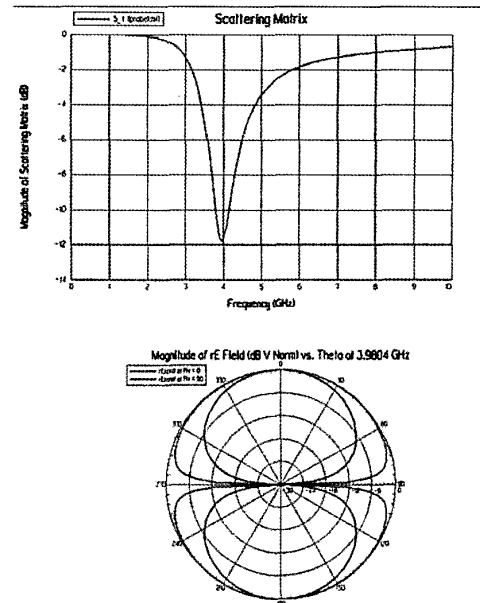


Figure 14. a) S_{11} of the antenna with all the switches disconnected (OFF). The antenna functions as a bowtie at around 4GHz. b) Radiation pattern at around 4GHz (dipole-like), and antenna's characteristics.

When all the switches are connected (ON), the antenna functions with its full-size, and it resonates in different frequencies, and especially at 2.19GHz as shown in Fig. 15.

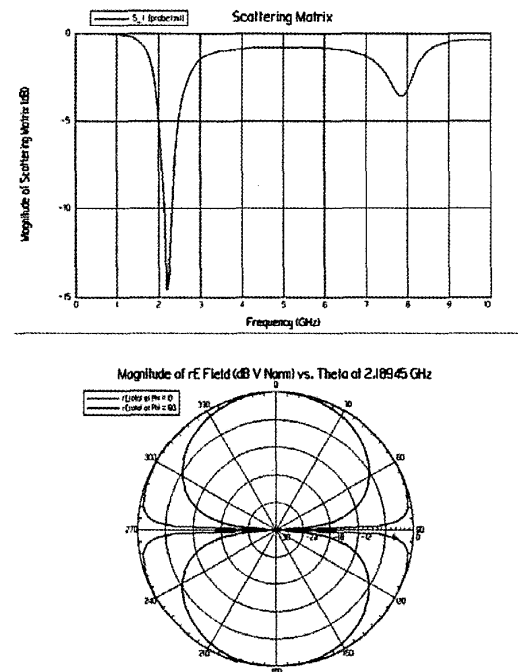


Figure 15. a) S_{11} of the antenna with all the switches connected (ON). The antenna functions as a bowtie at around 2.19GHz as expected. b) Radiation pattern at 2.19 GHz.

IV. THz ANTENNAS USING MICROMACHINING

Micromaching can also be used to fabricate 3-Dimensional structures, such as helical antennas, singular and arrayed, for the millimeter and THz range. The THz antenna structures are fabricated by using Laser Chemical Vapor Deposition (LCVD) to form fibers that can be grown into complex three-dimensional structures directly on semiconductor substrates.

Figure 16, shows a cw laser beam focused onto a substrate, with intensity sufficient to achieve high temperature and initiate the deposition process. Reduced laser power may be required as the fiber begins to grow, since heat loss from the laser-heated region decreases as the fiber grows away from the substrate.

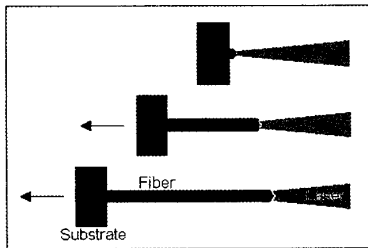


Figure 16. Micromachining Fiber growth

By focusing the laser through a diffractive optic, arrays of antennas can be fabricated at the same time, as shown in Figure 17. THz radiation detection devices can be realized by combining the helical antennas with MEMS microbolometers that convert received THz radiation into a change in resistance.

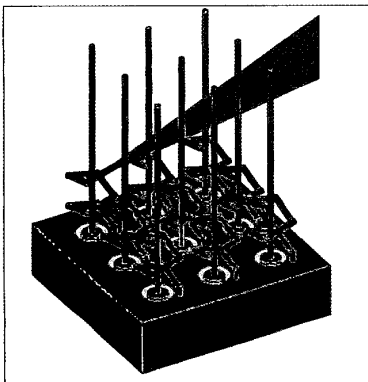


Figure 17. An array of MEMS helical antennas

Figure 18 shows an SEM Photograph of an Antenna-Like Structure Consisting of 40µm square Spirals Around a Center Post.

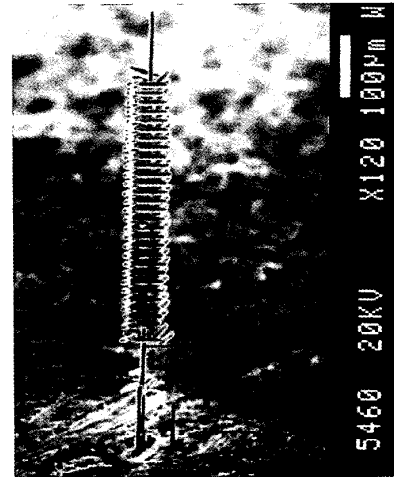


Figure 18. A MEMS helical antenna

Several applications can be realized by combining these antenna structures with other THz MEMS devices, such as THz waveguides, and with devices such as bolometers and diode harmonic mixers [13-16]. One application is a high frequency spectrum analyzer. Arrays of antennas, dipole or helical, could be fabricated on the same substrate to monitor frequencies from 100GHz to over 2THz. Each antenna would have a calibrated bolometer matched to its impedance. The output voltages would represent the signal levels present at discrete frequency bands. Another application would be a high-resolution scanner chip operating in the far-infrared (FIR) frequency band. Arrays of micro helical antennas would be used, possible with FIR optical lenses, to produce such a camera. Arrays of these antenna-bolometer pairs can be fabricated on the same substrate to realize a THz imaging device shown in Figure 19.

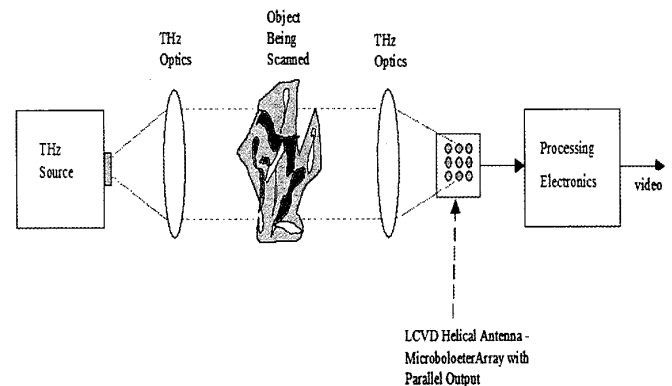


Figure 19. A THz Imager using MEMS Helical Antenna Technology

V. CONCLUSIONS

A new approach to multiple frequency fractal antennas using RF MEMS switches was presented. Instead of utilizing only the resonance frequencies offered to the designer by the nature of the fractal antennas, additional resonances can be achieved by making use of RF MEMS switches. The placement of each switch can control the current on each conductive part of a fractal antenna. That affects the resonance behavior of the entire antenna and its radiation pattern. Several other fractal antennas such as the Sierpinski gasket antenna can be used in conjunction with RF MEMS switches to create a re-configurable and more versatile antenna. Such an approach to re-configurable antennas permits deliberate alterations in antenna performance to accommodate changes in mission, environment; tolerance to defects and faults in modern communication systems. Also shown in this paper is how dipole and helical microstructures can be fabricated as singular structures and in arrays. Several applications can be realized by combining these antenna structures with other THz MEMS devices, such as THz waveguides, and with devices such as bolometers and diode harmonic mixers.

REFERENCES

- [1] R. J. Richards and De Los Santos H J, *MEMS for RF/microwave wireless applications: the next wave*. Microwave J., 2001, No. 44, pp. 20–41
- [2] H. J. De Los Santos and Richards R J, *MEMS for RF/microwave wireless applications: the next wave. Part II*. Microwave J., 2001, No. 44, pp. 142–152.
- [3] A. Borgioli, Liu Y, Nagra A. S. and York R. A., *Low-loss distributed MEMS phase shifter*, IEEE Microw. Guid. Wave Lett, 2000, No. 10, pp. 7–9.
- [4] K. Grenier, Barber B P, Lubecke V, Zierdt M, Safar H, Pons P and Gammel P L, *Integrated RF MEMS for single chip radio Transducers '01—EUROSENSORS XV (Munich, Germany, 10–14 June 2001)*, pp 1528–31.
- [5] H. A. C. Tilmans, W. De Raedt and E. Beyne, MEMS for wireless communications: 'from RF-MEMS components to RF-MEMS-SiP', Journal of Micromech. Microeng., vol. 13, 2003, S139–S163.
- [6] D. Anagnostou, C.G. Christodoulou, and J.C. Lyke, *Re-configurable Array Antennas for Wideband Applications*, IEEE Aerospace Conference, March. 2002
- [7] J. Gianvittorio, Y. Rahmat-Samii, *Fractal Element Antennas: A Compilation of Configurations with Novel Characteristics*, Antennas and Propagation for Wireless Comms. 2000, IEEE-APS Conference, pp. 129–132
- [8] C. Puente, J. Romeu, R. Pous, X. Garcia, F. Benitez, *Fractal multiband antenna based on the Sierpinski gasket*, Electronics Letters, Volume: 32 Issue: 1, 4 Jan. 1996, Page(s): 1–2
- [9] J. Romeu, J. Soler, *Generalized Sierpinski fractal multiband antenna*, Antennas and Propagation, IEEE Transactions on, Volume: 49 Issue: 8, Aug. 2001, Page(s): 1237–123
- [10] C. Puente-Baliarda, J. Romeu, R. Pous, A. Cardama, *On the behavior of the Sierpinski multiband fractal antenna* Antennas and Propagation, IEEE Trans., Vol.46 Issue: 4, April 1998 pp. 517–524
- [11] D. Anagnostou, M. Khodier, J. Lyke, C. Christodoulou, *Fractal antenna with RF-MEMS switches for multiple frequency applications*, Antennas and Propagation Society International Symposium, 2002, IEEE, Volume: 2, 2002, pp. 22–25
- [12] D. Anagnostou, *Fractal Antennas with RF-MEMS Switches*, Masters Thesis, University of New Mexico, Electrical and Computer Engineering Dept, December 2002.
- [13] L. P. B. Katehi, G. M. Rebeiz, T. M. Weller, R. F. Drayton, H. -J. Cheng and J. F. Whitaker, "Micromachined Circuits for Millimeter- and Sub-millimeter-Wave Applications," IEEE Antennas and Propagation Magazine, Vol. 35, No. 5, pp.9-17, October 1993.
- [14] M. Boman, H. Westberg, S. Johansson, J.-Å. Schweitz, Proc. 5th International Workshop on Micro Electro Mechanical Systems, 4-7 Feb. 1992, Travemünde, Germany.
- [15] A. G. Cha, "Wave Propagation on Helical Antennas," IEEE Transactions Antennas and Propagation, Vol AP-20, Sept. 1972.
- [16] R. N. Dean, Jr., P.C. Nordine and C. G. Christodoulou, "3-D Helical THz Antennas", *Microwave and Optical Technology Letters*, pp. 106-111, Jan. 20, 2000

Christos G. Christodoulou received his Ph.D. degrees in Electrical Engineering from North Carolina State University, Raleigh, in 1985. He served as a faculty member in the University of Central Florida, Orlando, from 1985 to 1998, where he received numerous teaching and research awards. In 1999, he joined the faculty of the Electrical and Computer Engineering Department of the University of New Mexico, Albuquerque as a Chair. In 1991 he was selected as the AP/MTT Engineer of the year (Orlando Section). He is Fellow member of IEEE and a member of URSI (Commission B). He served as the general Chair of the IEEE Antennas and Propagation Society/URSI 1999 Symposium in Orlando, Florida and the co-chair of the IEEE 2000 Symposium on Antennas and Propagation for wireless communications, Waltham, MA. He has published over 170 papers in journals and conferences. He also has two patents. He is, currently, the co-editor for a column on "Wireless Communications" for the IEEE AP Magazine, and an associate editor for the IEEE Transactions on Antennas and Propagation and the ACES journal. His research interests are in the areas of wireless communications, smart antennas, neural network applications in electromagnetics, and MEMS antennas.